A single-crystal Electron Paramagnetic Resonance study at 95 GHz of the type 1 copper site of the green nitrite reductase of Alcaligenes faecalis

Gastel, M. van; Boulanger, M.J.; Canters, G.W.; Huber, M.I.; Murphy, M.E.P.; Verbeet, M.P.; Groenen, E.J.J.

A Single-Crystal Electron Paramagnetic Resonance Study at 95 GHz of the Type 1 Copper Site of the Green Nitrite Reductase of *Alcaligenes faecalis*

M. van Gastel,[†] M. J. Boulanger,[‡] G. W. Canters,[||] M. Huber,[†] M. E. P. Murphy,[⊥] M. Ph. Verbeet,[||] and E. J. J. Groenen*,[†]

Centre for the Study of Excited States of Molecules, Huygens Laboratory, Leiden University, P.O. Box 9504, 2300 RA Leiden, The Netherlands, Department of Biochemistry and Molecular Biology, University of British Columbia, Vancouver BC V6T 1Z3, Canada, Department of Chemistry, Gorlaeus Laboratories, Leiden University, P.O. Box 9502, 2300 RA Leiden, The Netherlands, Department of Microbiology and Immunology, University of British Columbia, Vancouver BC V6T 1Z3, Canada

Received: August 2, 2000; In Final Form: December 11, 2000

An electron-spin-echo−detected electron paramagnetic resonance (EPR) study has been performed for the type 1 copper site of the green nitrite reductase of *Alcaligenes faecalis*. Accurate *g* values and principal directions of the *g* tensor have been obtained. The *z* principal axis of the *g* tensor makes an angle of 60° with the direction from copper to the Sδ of the axial methionine. The direction of this axis is compared with that of the blue type 1 proteins azurin and M121Q azurin and of the green type 1 protein M121H azurin, and interpreted in terms of the d orbital at copper in the wave function of the unpaired electron. This d orbital is oriented such that the overlap with the lone-pair orbitals of the ligands is maximum. The relation between the absorption spectrum in the visible, the copper−thiolate interaction, and the rhombicity of the EPR spectrum of type 1 proteins is discussed in terms of the trigonal and tetragonal character of the copper sites and the position and strength of the axial ligand.

Introduction

To deepen our level of understanding of the biological activity of enzymes, information is needed concerning the electronic properties of the catalytically active sites. Spectroscopic studies of the metal site in copper-containing electron-transfer proteins have shown that structurally similar sites may show profound differences in their electronic structure. Within the family of type 1 copper sites, for example, both the ratio of the absorption at 450 and 600 nm and the rhombicity of the electron paramagnetic resonance (EPR) spectrum vary significantly.[1] A particularly intriguing case concerns the copper-containing nitrite reductases of different origin. The nitrite reductases of *Alcaligenes xylosoxidans* and *Pseudomonas aureofaciens* are blue and have axial EPR spectra, whereas the nitrite reductases of *Alcaligenes faecalis* strain *S6*, *Achromobacter cycloclastes*, and *Rhodobacter sphaeroides* are green and have rhombic EPR spectra.[2,3] To investigate these differences we have performed high-frequency pulsed EPR spectroscopy. The use of 95 GHz instead of the common 9 GHz microwave frequency provides a better resolution and has enabled the study of a single crystal of *A. faecalis S6*.

Nitrite reductase has a trimeric structure and contains two types of copper sites.[4] In the catalytic cycle of these proteins, the so-called type 2 site, in which the copper is ligated by three histidines and a water molecule, binds the nitrite at the expense of water. Subsequently, the nitrite is reduced once an electron is obtained from the other copper site,[5,6] a type 1 site in which the copper is ligated by two histidines, a cysteine, and a methionine. In the crystal of *A. faecalis* nitrite reductase, the distance between the coppers is approximately 13 Å with a histidine and a cysteine residue between.[5,7] The type 1 site is shown in Figure 1. The copper is about 0.5 Å out of the plane spanned by the Nδ atoms of histidines 95 and 145 and the Sγ of cysteine 136 (the NNS plane). The distance of copper to these atoms is about 2.1 Å, and the distance of copper to the Sδ of methionine 150 is about 2.7 Å. The distance of copper to the NNS plane is larger than for the type 1 blue-copper proteins plastocyanin of *P. nigra* (0.34 Å[8]) and azurin of *Pseudomonas aeruginosa* (0.08 Å[9]), whereas the copper to Sδ bond length is slightly shorter than that for plastocyanin (2.8 Å) and azurin (3.1 Å). For the latter proteins, the blue color arises from an intense absorption at about 600 nm, which has been ascribed to a charge-transfer transition from the Sγ of the cysteine to copper.[10] The green color of *A. faecalis* nitrite reductase arises from an increased absorption at about 450 nm compared with that for the blue type 1 sites. This increase has been correlated to a coupled angular movement of the cysteine and methionine residues toward a more flattened tetrahedral structure.[11,12]

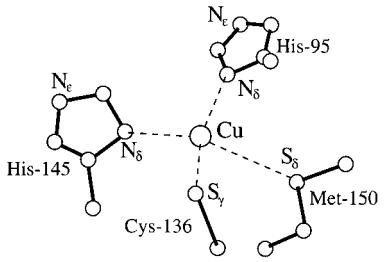

Figure 1. The type 1 copper site of *A. faecalis* nitrite reductase.[5]

In this article we report the results of an electron-spin-echo (ESE)−detected EPR study of a single crystal of *A. faecalis*

[†] Huygens Laboratory, Leiden University.
[‡] Department of Biochemistry and Molecular Biology, University of British Columbia.
[||] Gorlaeus Laboratories, Leiden University.
[⊥] Department of Microbiology and Immunology, University of British Columbia.

10.1021/jp002761u CCC: $20.00
Published on Web 02/22/2001

nitrite reductase. The complete *g* tensor has been determined for the type 1 site and interpreted in relation to the d orbital at copper occupied by the unpaired electron. The *z* principal axis of the *g* tensor is neither perpendicular to the NNS plane, nor to the CuNN plane. We have analyzed the orientation of the *z* axis of the *g* tensor and compared it with that for azurin and two of its mutants, M121Q and M121H azurin. A model is formulated that predicts the orientation of the d orbital at copper in the wave function of the unpaired electron. This orbital appears to be oriented such that the overlap with the lone-pair orbitals of the ligands is maximized.

Materials and Methods

Sample Preparation. The expression and purification procedure for *A. faecalis* nitrite reductase is described in ref 13. Crystallization of nitrite reductase is performed using reservoir solutions of 6−12% poly(ethylene glycol) 6000, 0.1 M sodium acetate at pH 4.5−5.5. The crystallization drops consist of equal volumes of reservoir solution and protein solution of 10 mg/mL nitrite reductase in 10 mM Tris-HCl at pH 7. The crystals have typical dimensions of $0.1 \times 0.1 \times 0.1$ mm^3 and are transferred in a reservoir solution of pH 5.0.

EPR Spectroscopy. The EPR experiments were performed at a temperature of 1.2 K on a home-built ESE spectrometer at 95 GHz. The spectrometer is described in ref 14, except that the microwave bridge was replaced by one from the Department of Microwave Equipments for Millimeter Waveband ESR Spectroscopy in Donetsk, Ukraine. A nitrite reductase crystal was mounted in a capillary tube with an inner and outer diameter of 0.60 and 0.84 mm, respectively, and the edges of the tube were closed with sealing wax. The electron spin echoes are generated by a two-pulse sequence with typical pulse lengths of 60 and 120 ns, respectively, and a pulse separation of 300 ns, at a repetition rate of 10 Hz. The intensity of the echo is recorded by a boxcar integrator and fed into a computer via an ADC. The EPR spectrum for each orientation of the magnetic field with respect to the nitrite reductase crystal is recorded by monitoring the height of the echo while scanning the strength of the magnetic field. Because the spectrometer allows for a rotation of the direction of the magnetic field in a plane that contains the capillary tube and a rotation of the capillary about its own axis, all orientations of the magnetic field with respect to the crystal could be selected without remounting the crystal.

Calculations. For the model presented in section A of the discussion, the overlap between the copper d orbital in the wave function of the unpaired electron and the ligands orbitals has been obtained as follows. The coordinates of the atoms were taken from the X-ray data. The overlap integrals were calculated numerically by approximating the 3d orbital at copper by a Slater d orbital ($Z_{\text{eff}} = 13.75$), the lone-pair orbitals at the nitrogens by sp^2-hybridized Slater orbitals ($Z_{\text{eff}} = 3.9$) oriented such that their C_∞ axes are in the respective imidazole planes and bisect the Cγ−Nδ−Cϵ angle, and the lone-pair orbital at sulfur of the cysteine by a Slater p orbital ($Z_{\text{eff}} = 5.45$) oriented such that its C_∞ axis is perpendicular to the Sγ(Cys)−Cu direction and makes an angle of 109° with the Sγ(Cys)−Cβ(Cys) direction. For all proteins under consideration, the C_∞ axis of the latter orbital turned out to be within 20° of the NNS plane, and the description in terms of a p orbital was based on quantum-chemical calculations, in which no s character at sulfur is found in the singly occupied molecular orbital.[10] The lone-pair orbitals at the sulfur of the methionine are approximated by Slater sp^3 orbitals ($Z_{\text{eff}} = 5.45$) such that the C_∞ axes of both lone-pair orbitals are in the plane perpendicular to the CγSδCϵ plane and that the sulfur has an approximately tetrahedral electronic configuration. The orbital for which the C_∞ axis points closest to copper has been selected. For the M121Q mutant of azurin, which has a glutamine at the axial position, the lone-pair orbital at the Oϵ of the glutamine is approximated by a Slater sp^2 orbital ($Z_{\text{eff}} = 4.55$) with its C_∞ axis pointing from oxygen to copper. For the M121H mutant of azurin, which has a histidine at the axial position, the lone-pair orbital at the Nδ of the axial histidine was approximated in the same way as the strongly ligated histidines. A grid around copper of $6 \times 6 \times 6$ Å^3 and $81 \times 81 \times 81$ gridpoints was used to calculate the overlap integrals of the 3d orbital with the respective ligand orbitals. The total overlap was calculated by summing the absolute values of the individual overlap integrals with equal weight. The orientation of the 3d orbital at copper was initially set parallel to the CuNN plane and varied until an orientation was found for which the overlap is maximum.

Results

ESE-detected EPR spectra at 95 GHz and 1.2 K of a single crystal of *A. faecalis* nitrite reductase recorded for different orientations of the magnetic field $\vec{B}_0$ with respect to the crystal are shown in Figure 2. The spectra depend strongly on the direction of $\vec{B}_0$ and comprise numerous bands that overlap considerably. Intense bands are observed in the area between 3.05 and 3.35 T, weak ones at lower fields. The latter derive from the type 2 site and will not be considered further in this section. For $\vec{B}_0$ parallel to a crystal axis, several resonances coincide and the intensity concentrates in a limited number of bands (see Figures 2g, 2h, and 2i).

The single crystal of nitrite reductase belongs to space group $P2_12_12_1$ with four asymmetric units per unit cell.[7] Each asymmetric unit contains one nitrite reductase molecule, a trimer that consists of three identical monomeric subunits connected by a 3-fold rotation axis. Each monomer contains one type 1 and one type 2 copper site. With 12 type 1 copper sites in the unit cell, the EPR spectrum comprises 12 resonances for an arbitrary orientation of $\vec{B}_0$ with respect to the crystal. One of the fields of resonance becomes stationary when the magnetic field is aligned along a principal *x* (*z*) axis of a *g* tensor, corresponding to the smallest (largest) *g* value, respectively. We have determined the orientations of the principal *x* axes with respect to a laboratory axis system, by looking for directions of $\vec{B}_0$ for which a resonance occurs at the extreme high-field side of the spectrum, that is, a direction for which this resonance shifts to lower field for any change in the direction of $\vec{B}_0$. In this way, the orientations of 12 *x* axes have been established with an accuracy of 4°. All spectra for which $\vec{B}_0$ is parallel to an *x* axis contain a resonance at 3.345 T ($g_{xx} = 2.026$). The 12 *x* axes form three groups of four, for which the corresponding spectra within each group are identical. The three distinct spectra are shown in Figures 2a, 2c, and 2e. Similarly, the orientations of 12 *z* axes have been established with the same accuracy as the *x* axes by looking for directions $\vec{B}_0$ for which the EPR spectrum contains a resonance at the extreme low-field side of the spectrum. This low-field resonance occurs at 3.090 T ($g_{zz} = 2.195$), and the *z* axes are also divided into three groups of four, for which the corresponding spectra within each group are identical. Each *z* axis is perpendicular to an *x* axis within 2°. The three distinguishable spectra for which $\vec{B}_0$ is parallel to a *z* axis are represented in Figures 2b, 2d, and 2f.

Subsequently, the directions of the crystallographic axes have been determined. These axes are 2-fold screw axes that relate

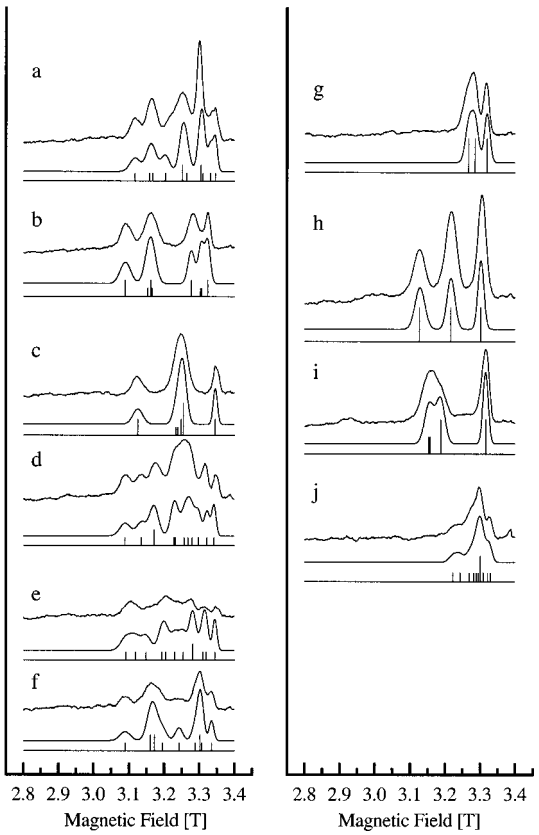

Figure 2. ESE-detected EPR spectra of a single crystal of *A. faecalis* nitrite reductase for different orientations of the magnetic field with respect to the crystal. Upper traces, experimental spectra; middle traces, simulated spectra; lower traces, stick spectra that indicate the fields of resonance of the 12 molecules in the unit cell. The simulated spectra are derived by dressing the sticks with a Gaussian line width (cf., data analysis). Sticks have been drawn on top of each other when resonances were calculated within 3 mT. Within 1°, the spectra in panels a, c, and e correspond to the orientation of the magnetic field parallel to the *x* principal directions of the three monomers in the same asymmetric unit; those in panels b, d, and f, to the *z* principal directions of the monomers in the same asymmetric unit; those in panels g, h, and i, to the crystallographic *a*, *b*, and *c* axes; and that in panel j, to the a C_3 axis. The low-intense and narrow band at high field ($B = 3.385$ T and $g = 2.0028$) derives from the sealing wax.

four monomers, one in each asymmetric unit. The four *x* (and *z*) axes of those monomers are consequently related by 2-fold rotations about the crystallographic axes. Approximate directions of the crystallographic axes are derived from the orientations of these axes. These directions have been optimized by looking for nearby orientations of $\vec{B}_0$ for which the number of bands in the spectrum and the width of the bands is minimum. When the magnetic field is aligned with a crystallographic axis, the four symmetry-related monomers become magnetically equivalent. As a result, three distinct resonances of the type 1 sites appear in the EPR spectrum. The spectra for which $\vec{B}_0$ is parallel to a crystallographic axis are shown in Figures 2g, 2h, and 2i.

The directions of the C_3 rotation axes of the trimers have been determined. A C_3 axis relates the monomers within one trimer and the corresponding *g* tensors by a 120° rotation. When $\vec{B}_0$ is aligned with a C_3 axis, the monomers of that trimer are magnetically equivalent and 10 bands are expected in the EPR spectrum, one with approximately triple intensity and nine from the other monomers. From the 3-fold symmetry present among the 12 *x* and *z* axes, four approximate directions of the C_3 axes have been constructed. The C_3 axes, like the *x* and *z* axes, are related by 2-fold rotations about the crystallographic axes, and the corresponding EPR spectra are identical. An EPR spectrum for which $\vec{B}_0$ is parallel to a C_3 axis is shown in Figure 2j.

A summary of the directions of all *x* and *z* axes and the C_3 axes with respect to the crystallographic axes *a*, *b*, and *c* is shown in the Wulffnet projections of Figure 3 . (For the identification of the crystallographic axes, see Data Analysis, section B.) A dot indicates that a direction points to the back of the sphere. In Figure 3a, the 2-fold symmetry of the *abc* axes is emphasized, and the *x* and *z* axes that are interrelated by the 2-fold rotations are indicated with symbols of the same thickness. Three groups of four *x* and *z* axes are present. In Figure 3b, the 3-fold symmetry of the C_3 axes is emphasized, and this time the *x* and *z* axes that are interrelated by the 3-fold rotations around the C_3 axes are indicated with symbols of the same thickness. In this way, four groups of three *x* and *z* axes are formed for which the axes within a group stem from one trimer.

During the measurements, a large number of EPR spectra have been recorded at many directions of $\vec{B}_0$. About 50 of those spectra, chosen because their directions cover the complete unit sphere, have been included in the refinement procedure (see Data Analysis, section A) along with the spectra that correspond to the experimentally determined directions of the *x* and *z* axes and the crystallographic axes, to enhance the accuracy of the experimentally found directions of the *x*, *z*, crystallographic, and C_3 axes.

Data Analysis

A. The ESE-Detected EPR Spectra. To refine the principal *g* values and the directions of the principal axes, the ESE-detected EPR spectra have been simulated. For a particular orientation of $\vec{B}_0$ with respect to the crystal, the fields of resonance of each monomer in the unit cell are calculated according to

$$B_{\mathrm{res}} = \frac{h\nu}{\mu_\beta \sqrt{\sum_i (g_{ii} \cos \phi_i)^2}} \qquad (1)$$

where $i = x, y, z$, h is Planck's constant, ν is the microwave frequency, μ_β is the Bohr magneton, and ϕ_i is the angle between the axis i of the *g* tensor of the particular monomer and $\vec{B}_0$. Copper hyperfine interaction was not explicitly taken into account, because it is not resolved in the ESE-detected EPR spectra at 95 GHz. The calculated resonances are fit to the resonances observed in a large number of EPR spectra recorded for different orientations of $\vec{B}_0$ with respect to the crystal. The g_{ii} values and the angles ϕ_i are optimized in a nonlinear least-squares fit with restrictions set by the symmetry of the space group, such that the calculated resonances of the type 1 sites are in good agreement with the bands observed in the experimental spectra. In this way, 12 refined *g* tensors, 3 refined directions of the crystallographic axes, and 4 refined directions of the C_3 axes are found with an accuracy of 1 degree. All directions are within 3° of the directions determined in the experiment. The refined *g* values, shown in Table 1, are nearly identical with the *g* values read from the spectra.

The calculated fields of resonance for the orientations of $\vec{B}_0$ in Figure 2 are included as sticks underneath the experimental spectra in Figure 2. To facilitate comparison with the experi-

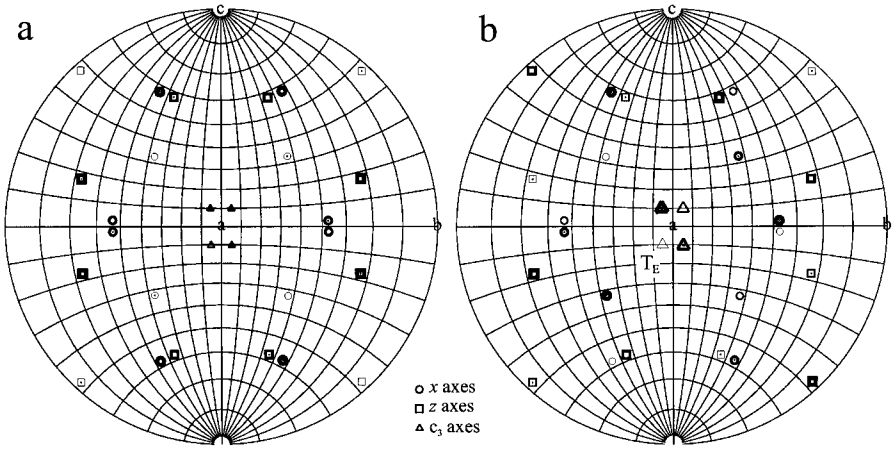

Figure 3. Wulff stereoprojection of the principal *x* and *z* directions of the *g* tensor of the 12 molecules in the unit cell. The crystallographic axes are used as a reference, where the *a* axis points to the front, the *b* axis to the right, and the *c* axis upward. The circles correspond to *x* directions, the squares correspond to *z* directions, and the triangles indicate the directions of the C_3 axes. A dot in the symbol indicates that the direction points toward the back of the sphere. In a, the principal axes of the monomers that are related by 2-fold rotations around the crystallographic axes are indicated by symbols of the same thickness. In b, the principal axes of the monomers of the same trimer are indicated by symbols of the same thickness. The C_3 axis denoted by T_E belongs to the trimer specified in the pdb file.

TABLE 1: Refined *g* Values and Direction Cosines of the Principal Axes (*xyz, x′y′z′, x″y″z″*) of the *g* Tensors of the Type 1 Copper Site of *A. faecalis* Nitrite Reductase[a]

	$g_{xx} = 2.0264 \pm 0.0003$				$g_{yy} = 2.0509 \pm 0.0017$				$g_{zz} = 2.1951 \pm 0.0003$		
	a	b	c		a	b	c		a	b	c
x	0.6091	−0.7928	0.0222	*x′*	0.6429	0.5410	−0.5422	*x″*	0.2732	0.3756	0.8856
y	0.6403	0.5081	0.5761	*y′*	0.7616	−0.5272	0.3769	*y″*	0.9116	0.1930	−0.3631
z	−0.4680	−0.3367	0.8171	*z′*	−0.0819	−0.6553	−0.7509	*z″*	−0.3073	0.9065	−0.2897
T_E	0.9664	0.0825	0.2433								
T_X	0.9808	0.0818	0.1772								

[a] The directions of the *g* axes are specified in the crystallographic axis system (*abc*). The three *g* tensors (unprimed, singly primed, doubly primed) correspond to the three monomers of the trimer specified by the X-ray data (pdb file 1AS7 [5]). Included in the table is the direction of the 3-fold axis of the trimer, determined by EPR (T_E) and X-ray crystallography [5] (T_X).

mental spectra, each stick is dressed with a Gaussian line shape of width

$$\Delta B = \sqrt{\sum_i (W_{ii} \cos \phi_i)^2} \qquad (2)$$

where W_{ii} are the principal values of the line width tensor. The principal directions of the line width tensor are assumed to be parallel to those of the corresponding *g* tensor. The dressed spectra are included in Figure 2 as middle traces in each panel. Relaxation and modulation effects that derive from the ESE technique and influence the intensity of the bands are not taken into account in the simulations. The positions of the bands in the experimental spectra agree nicely with those in the simulated spectra. Values of 6 mT, 9 mT, and 15 mT are found for W_{xx}, W_{yy}, and W_{zz}, respectively. The larger value of W_{zz} compared with those of W_{xx} and W_{yy} indicates that the line width not only derives from *g* strain but also includes the unresolved copper hyperfine interaction.[15,16]

B. Identification of the Crystallographic Axes. Usually, the EPR experiment allows the determination of the directions of the crystallographic axes, but for their identification an additional X-ray diffraction experiment on the mounted crystal is necessary. EPR suffices in the present case. The orientation of the 3-fold axis of the trimer provides additional information that is sufficient to establish which crystallographic axis is which. In Table 1, the direction of the 3-fold axis T_X, determined by X-ray diffraction for the trimer specified in the Protein Data Bank (pdb) file 1AS7,[5] is given in the *abc* crystallographic axes system. As is seen from its components, this vector is nearly parallel to the crystallographic *a* axis. The four C_3 axes found in the EPR experiment are also close to a crystallographic axis (cf. Figure 3), which is thereby identified as the *a* axis. Based on the correspondence between the orientation of T_X and T_E, one of the 3-fold axes as determined from EPR, the other two crystallographic axes are identified as *b* and *c* (cf. Table 1). The average angle between the directions of the trimer axes determined by X-ray diffraction and by EPR is 4°, within the combined accuracy of the experiments.

C. Orientation of the *g* Tensor with Respect to the Type 1 Copper Site. From the EPR data, the orientation of the three principal axes systems of the *g* tensors that are related by the 3-fold axis T_E, and stem from the trimer in the asymmetric unit specified in the pdb file,[5] have been fixed with respect to the crystallographic *a*, *b*, and *c* axes. The *g* axes are denoted by *xyz*, *x′y′z′*, and *x″y″z″* and their components along the *a*, *b*, and *c* axes are given in Table 1. To derive the orientation of the *g* axes within the nitrite reductase molecule, in particular with respect to the copper site, we use the structure of the asymmetric unit as determined from X-ray diffraction. Three assignments are possible such that the orientation of the *g* tensor axes with respect to the type 1 copper site is the same for each monomer. These are presented in Table 2. Consideration of the electronic structure of the copper site allows elimination of two of these.

The electronic structure of the type 1 sites of several proteins has been calculated by self-consistent-field scattered-wave methods[11,17−19] and the orientation of the principal axes of the *g* tensor is known for the blue-copper protein azurin[15] and its mutants M121Q[16] and M121H.[20] In the calculations, the singly occupied molecular orbital contains a d orbital at copper that is

TABLE 2: Angles between the Directions of the Principal Axes of the *g* Tensors and the Bond Directions from Copper to Its Ligands for the Type 1 Copper Site of Monomer A (Nomenclature According to the X-ray structure, pdb file 1AS7[5])[a]

	x	*y*	*z*	*x′*	*y′*	*z′*	*x″*	*y″*	*z″*
CuNδ(His-95)	15°	86°	104°	108°	150°	114°	93°	99°	9°
CuSγ(Cys-136)	146°	76°	120°	121°	38°	69°	84°	33°	123°
CuNδ(His-145)	94°	163°	76°	54°	109°	43°	43°	128°	104°
CuSδ(Met-150)	80°	32°	60°	82°	74°	162°	175°	94°	87°
CuNδNδ plane			71°			39°			8°
NδNδSγ plane			60°			43°			21°

[a] Also included are the angles between the *z*, *z′*, and *z″* axes and the planes spanned by copper and the copper-coordinated nitrogens of histidines 95 and 145 and by the nitrogens and the sulfur of cysteine 136 in monomer A.

π antibonding to a 3p orbital of the sulfur of the coordinated cysteine and σ antibonding to the lone-pair orbitals of the nitrogens of the histidines. The direction of the *z* axis, determined by spin−orbit coupling, is to good approximation perpendicular to the plane of maximum probability amplitude of the d orbital at copper. For azurin from *P. aeruginosa*, where the copper is almost in the equatorial plane spanned by the sulfur and the nitrogens (NNS plane),[9] the *z* axis is found perpendicular to this plane.[15] For the azurin mutants M121Q and M121H, where the axial methionine-121 has been replaced by a glutamine or a histidine, the copper is further from this plane and closer to the stronger axial ligand,[21,22] and the *z* axis is almost perpendicular to the plane spanned by copper and the copper-coordinated nitrogens of the histidines.[16,20] In all three cases, the *x* axis of the *g* tensor makes an angle of less than 20° with a copper−nitrogen bond.

The angles between the principal axes *xyz*, *x′y′z′*, *x″y″z″* and the bond directions from copper to its ligands in monomer A (nomenclature according to the pdb file 1AS7[5]) are shown in Table 2. Also included are the angles between the *z*, *z′*, and *z″* axes and the plane spanned by copper and the copper-coordinated nitrogens in monomer A. From the latter angles, it is clear that the *z* axis is closest to being perpendicular to this plane, making an angle of 71°. Furthermore, the *x* and *y* directions are close to the directions from copper to Nδ(His-95) and Nδ(His-145), respectively, making angles of 15° and 17°. Consequently, the *g* tensor specified by *xyz* most probably belongs to monomer A. Similarly, the *x′y′z′* and *x″y″z″* axes are assigned to monomers C and B, respectively, where they make the same angles with the copper-ligand directions as the *xyz* axes in monomer A. The resultant orientation of the *g* tensor axes for the type 1 copper site in green nitrite reductase is pictorially reported in Figure 4.

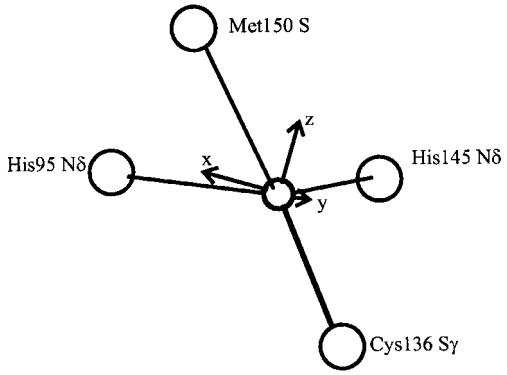

Figure 4. The principal directions of the *g* tensor with respect to the type 1 copper site.

Discussion

The high resolution and sensitivity of EPR spectroscopy at 95 GHz compared with 9 GHz has allowed a quantitative EPR study of single crystals of nitrite reductase. The intense bands in the ESE-detected EPR spectra in Figure 2 derive from the type 1 copper site. This assignment is based on the experimental value of g_{zz}, which is known from EPR experiments at 9 GHz.[7] The weak features at the low-field side of the ESE-detected EPR spectra, for example, at about 2.93 T in Figure 2i, are assigned to the type 2 copper site.

For the type 1 site, the dependence of the 12 intense bands on the orientation of the magnetic field allows the determination of the directions of the principal axes of the *g* tensor of all monomers in the unit cell with respect to the crystallographic axes. Combination with the structural data from X-ray crystallography subsequently yields the directions of the principal axes of the *g* tensor in the type 1 site. With the copper in the origin of the axes system, the *x* axis points approximately toward the Nδ(His-95), the *y* axis approximately toward Nδ(His-145). The *z* axis makes an angle of 19° with the normal to the CuNN plane. The value of g_{zz} (2.1951) is comparable with that of cucumber basic protein and somewhat smaller than for azurin, amicyanin, plastocyanin, and stellacyanin.[1] The rhombicity of the *g* tensor (i.e., $g_{yy} - g_{xx}$) amounts to 0.025, a little larger than for azurin,[15] amicyanin, and plastocyanin,[10] but smaller than for stellacyanin and cucumber basic protein.[1]

The low intensity of the bands that correspond to the type 2 site does not allow a reliable analysis of their orientational dependence. The resonance at 2.93 T in Figure 2i corresponds to a *g* value of about 2.31, compatible with the g_{zz} value reported for the type 2 site of nitrite reductase.[7] The weakness of the bands may be caused by different relaxation times of the type 2 and the type 1 sites or partial occupation or reduction of the type 2 site. To check the first hypothesis, the relaxation times of both copper sites in nitrite reductase were estimated by a pulsed EPR experiment at 9 GHz on frozen solutions of native nitrite reductase and a mutant that only contains the type 2 site.[23] The relaxation times of both sites were similar ($T_2 \sim 750$ ns at 10 K). Assuming this also applies to the single crystal at W-band, this finding makes it unlikely that large differences in relaxation times cause the low intensity of the bands from the type 2 site. The occupation is checked by atomic absorption measurements, which reveal 1.7−2 copper atoms per monomer. Partial reduction of the type 2 site cannot be excluded, but a definitive answer as to why the intensity of the bands from the type 2 site is significantly lower than that of the type 1 site must still be determined.

A. The Orientation of the *z* Axis of the *g* Tensor. The complete *g* tensor of the type 1 copper site has been obtained from the EPR study (cf. Tables 1 and 2). A quantitative quantum-chemical analysis of the tensor is beyond the scope of this article. Here we will discuss a qualitative model that rationalizes the observed orientation of the principal *z* axis of the *g* tensor. The *z* axis of the *g* tensor of nitrite reductase makes an angle of 71° with the CuNN plane (cf. Table 2). This orientation differs from that for azurin and its mutants M121Q and M121H. For the latter proteins, the *z* axis invariably is perpendicular to the CuNN plane, even though the distance of the sulfur of the cysteine to this plane varies considerably.

The model is based on the following ideas and assumptions. Assume that the part of the singly occupied molecular orbital that is localized on copper may be represented by a single 3d atomic orbital. This is in line with the results of density functional theory calculations, both for nitrite reductase[11] and

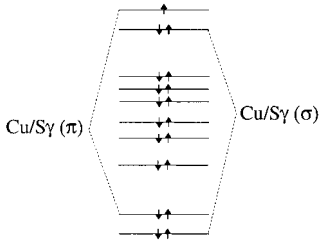

Figure 5. Schematic representation of the energy levels of the molecular orbitals with significant copper 3d character for plastocyanin (reproduced from ref 11). In the molecular orbitals that are lowest and highest but one in energy, the binding between Cu and S(Cys) is of σ and σ^* character. In those that are lowest but one and highest in energy, the binding between Cu and S(Cys) is of π and π^* character.

for plastocyanin.[24] The *z* axis of the *g* tensor is assumed to be perpendicular to the plane of maximum probability amplitude of this 3d orbital at copper. The 3d orbitals of an isolated copper ion are energetically degenerate. When the copper is coordinated by several ligands, the degeneracy is lifted. The eigenfunctions of the Hamiltonian become molecular orbitals that are linear combinations of copper 3d orbitals and ligand orbitals. We consider the subspace spanned by the molecular orbitals that contain a significant amount of 3d character at copper. Another basis for this subspace is formed by the 3d orbitals at copper and the relevant orbitals at the ligands. The expectation value of the Hamiltonian for an arbitrary wave function in this subspace is between the lowest and the highest of the eigenvalues corresponding to the eigenfunctions of the Hamiltonian. We assume that, upon binding, both the decrease in energy of a bonding orbital and the increase in energy of an antibonding orbital are proportional to the overlap between the copper and the ligand orbitals. According to this assumption, if it is known which ligand orbitals occur in the molecular orbital of lowest or highest energy, the part of the molecular orbital centered at copper is best approximated by looking for a copper orbital whose overlap with these ligand orbitals is maximum.

The idea is illustrated in Figure 5 where we have drawn a qualitative energy level scheme that corresponds to the subset of molecular orbitals with a significant copper 3d character as indicated by quantum-chemical calculations on blue-copper sites.[10−12,18,24−26] The molecular orbital of lowest energy concerns a 3d orbital at copper that is σ bonding to a 3p orbital at the sulfur of the cysteine. Following the assumptions of our model, we expect the copper orbital involved to be oriented such that the overlap with the sulfur orbital is maximum. Comparison of the X-ray structures of blue-copper proteins reveals that the angle Cβ(Cys)−Sγ(Cys)−Cu is conserved (109° for methionine as the axial ligand and 105° for glutamine as the axial ligand) irrespective of the position of the sulfur with respect to the CuNN plane. At an angle of 109° the 3p orbital at the sulfur of the cysteine points toward copper, which maximizes the overlap.

The model seems to work well for the bonding molecular orbital that has significant copper 3d character and is lowest in energy. What about the molecular orbital of highest energy with significant 3d character at copper? According to quantum-chemical calculations on the blue type 1 site of plastocyanin,[10,17,24,25] the molecular orbital of highest energy (cf. Figure 5), singly occupied, concerns a 3d orbital at copper which is π antibonding to a 3p orbital at the sulfur of the cysteine (different from the one involved in the σ bonding), and σ antibonding to the lone-pair orbitals at the coordinated nitrogens of the histidines. Calculations on the green type 1 site of nitrite reductase of *A. cycloclastes* [11,12] indicate that the bond between copper and the sulfur of the cysteine acquires σ-like antibonding character, wheras a lone-pair orbital of the axial ligand participates in the singly occupied molecular orbital as well. Consequently, to estimate the orientation of the d orbital present in the singly occupied molecular orbital, we searched for the orientation of a 3d orbital at copper such that the sum of the overlaps with the lone-pair orbital at the sulfur of cysteine, with the lone-pair orbitals at the nitrogens of the histidines and with the lone-pair orbital at the axial ligand is maximum. This was done numerically according to the procedure outlined in the materials and methods section. The orientation of the 3d orbital at copper was initially set parallel to the CuNN plane and varied until an orientation was found for which the overlap is maximum. This orientation is represented by the normal to the plane of maximum probability amplitude (called the *xy* plane) of the d orbital with maximum overlap (called d_{xy}).

TABLE 3: Angles between the Copper−Ligand Directions, the *z* Axis of the Experimental *g* Tensor and the z_{calc} Axis Corresponding to the d Orbital of Maximum Overlap[a]

	azurin		M121Q		M121H		nitrite reductase	
	z	z_{calc}	*z*	z_{calc}	*z*	z_{calc}	*z*	z_{calc}
CuNδ[a]	90°	94°	93°	94°	95°	96°	104°	105°
CuSγ(Cys)	97°	94°	108°	103°	126°	127°	120°	116°
CuNδ[b]	89°	88°	87°	93°	88°	85°	76°	84°
Cu(axial ligand)	15°	19°	10°	9°	41°	39°	60°	53°
$\angle(z, z_{calc})$	4°		6°		6°		8°	

[a] The directions of the *z* axes for azurin, M121Q and M121H are according to refs 15, 16 and 20, respectively. The atoms Nδ[a] and Nδ[b] belong to His-46 and His-117 for azurin, M121Q and M121H, and to His-95 and His-145 for nitrite reductase.

For azurin and its mutants M121Q and M121H, the orientation of the experimental *z* axis of the *g* tensor and the direction perpendicular to the calculated d_{xy} orbital, called z_{calc}, are given in Table 3. The directions of the *z* and z_{calc} axes differ on average by 6°, a small deviation in view of the simplifications of the model. The *z* and z_{calc} axes are almost perpendicular to the CuNN plane and make angles close to 90° with the copper−Nδ(His) directions. The d_{xy} orbital is almost in the CuNN plane, and two lobes point to the Nδ atoms of the coordinating histidines. For azurin the sulfur of the axial methionine is a weak ligand at a distance of 3.1 Å.[9] In accordance, the calculated overlap of the lone-pair orbital at the axial ligand with the d orbital at copper is small and of minor importance for the orientation of the d_{xy} orbital. For M121Q, the C_∞ axis of the lone-pair orbital at the Oϵ of the axial glutamine is about perpendicular to the CuNN plane, and the overlap of this lone-pair orbital with the d_{xy} orbital is almost zero. For M121H, the lone-pair orbital of the Nδ of the axial histidine is 45° away from the CuNN plane, and this orbital makes a small contribution to the total overlap.

When the model is applied to nitrite reductase, good agreement is found between the experimentally observed and the predicted direction of the *z* axis of the *g* tensor (cf. Table 3). Both the experimental *z* axis and the z_{calc} axis deviate from the normal to the CuNN plane and the directions of the *z* and z_{calc} axes differ by 8°. The direction of the *z* axis is in line with that found in the calculations on the copper site of nitrite reductase from *A. cycloclastes*,[11] assuming that the axis is perpendicular to the plane of maximum probability amplitude of the calculated d orbital in the wave function of the unpaired electron. If the lone-pair orbital at the sulfur of the cysteine is assigned more weight in the optimization process, based on the large coefficient of the orbital in the wave function of the unpaired electron, the agreement even improves. Apparently, the d orbital at copper

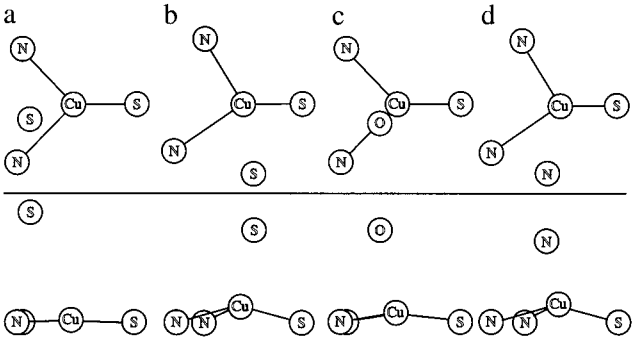

Figure 6. Schematic representation of the copper sites of *P. aeruginosa* azurin (a), *A. faecalis* nitrite reductase (b), M121Q azurin (c), and M121H azurin (d). The upper diagrams are projections onto the NNS equatorial plane, and the lower diagrams are side views parallel to the NNS plane and perpendicular to the Cu−S(Cys) direction.

in the wave function of the unpaired electron is oriented such that the sum of the overlaps with the lone-pair orbitals at the ligands is close to maximum.

B. The Optical Spectrum, the Copper−Thiolate Interaction, and the Rhombicity. In previous studies on nitrite reductase of *A. cycloclastes* by quantum-chemical methods,[11,12] the interaction between the copper and the sulfur of the cysteine in the wave function of the unpaired electron acquires σ-like character in contrast to that for the blue-copper protein plastocyanin, for which the interaction is predominantly of π character. The difference has been analyzed in ref 12 in terms of trigonal (π) and tetragonal (mainly σ) copper sites and quantified by the angle ϕ between the CuNN plane and the CuSS′ plane (CuSO for M121Q azurin and CuSN for M121H azurin). For an ideal trigonal structure ϕ is 90° and as ϕ decreases the site becomes tetragonal. The intense absorption at about 630 nm characteristic of trigonal sites and responsible for the blue color has been assigned to a charge-transfer transition corresponding to an excitation from the π bonding orbital to the singly occupied molecular orbital.[17] When ϕ decreases, an absorption at about 450 nm comes up, assigned to a charge-transfer transition corresponding to an excitation from the σ bonding orbital,[12] and changes the color of the protein to green. Azurin ($\phi = 83°$) and M121Q azurin ($\phi = 82°$) are blue; nitrite reductase ($\phi = 59°$) and M121H azurin ($\phi = 66°$) are green.

The π character of the copper−thiolate interaction for azurin and M121Q azurin and the partial σ character for nitrite reductase and M121H azurin, are predicted by the orientation of the d orbital of maximum overlap. Figure 6 shows schematic projections of the copper sites of azurin of *P. aeruginosa* (a), nitrite reductase of *A. faecalis* (b), M121Q azurin (c), and M121H azurin (d). The upper diagrams correspond to the projections onto the NNS plane, and the lower ones correspond to side views parallel to the NNS plane and perpendicular to the Cu−S(Cys) direction. For the trigonal structures of azurin and M121Q azurin, two lobes of the d orbital have σ interaction with the lone-pair orbitals at the nitrogens, and the other two lobes have π interaction with the orbital at the sulfur of the cysteine. For the tetragonal structures of nitrite reductase and M121H azurin, the nitrogens have slightly rotated around the normal to the NNS plane and the axial ligand has moved closer to the NNS plane. An equivalent way to formulate this structural variation is in terms of a coupled angular movement of the cysteine and methionine residues toward a more flattened structure.[11] Two lobes of the d orbital still have σ interaction with the nitrogens, but the interaction with the sulfur of the cysteine acquires σ character following the rotation of the nitrogens. In other words, one lobe of the d orbital turns toward the Cu−S(Cys) direction, whereas the other lobe acquires σ interaction with the axial ligand. The σ interaction between the d orbital and the lone-pair orbital at the axial ligand shows up in the calculations on nitrite reductase of *A. cycloclastes*, for which methionine character is found in the wave function of the unpaired electron.[11,12]

A generalized picture of the rhombicity of the *g* tensor in relation to the structure of type 1 copper proteins is lacking as yet. Contrary to the conclusion of previous theoretical work,[12] we find that the rhombicity and the angle ϕ do not seem to be correlated. Blue proteins may be axial or rhombic ($g_{yy} - g_{xx} = 0.017$ for azurin[15] and 0.054 for M121Q azurin[16]), and the same holds for green proteins (0.005 for M121H azurin[20] and 0.0245 for nitrite reductase). For proteins with weak axial ligands, like azurin and plastocyanin, the rhombicity is minor and seems to derive from the part of the wave function localized on sulfur.[10] When a stronger axial ligand is present, admixture of d_{z2} character may occur, which introduces rhombicity.[27] In calculations on stellacyanin, whose structural and spectroscopic properties are largely similar to those of M121Q azurin,[18] on cucumber basic protein and on nitrite reductase of *A. cycloclastes*, the admixture of d_{z2} character is comparable (depending on the method of calculation reported as 0.7%[11,18] or 3%[26]), but the EPR spectrum of nitrite reductase is significantly less rhombic (0.0245) than that of M121Q azurin (0.054 [16]). The d_{z2} character of the singly occupied molecular orbital for nitrite reductase may well be smaller than calculated. Alternatively, admixture of the d_{x2-y2} and d_{yz} (d_{xz}) orbitals may be responsible for the slightly increased rhombicity with respect to azurin.[20] For the green M121H azurin, the *g* tensor is virtually axial and the *z* axis of the *g* tensor and the direction from copper to the axial ligand make an angle of 41° (cf. Table 3). This observation led us to the conclusion that for M121H azurin the binding of the axial ligand probably involves the d_{yz} orbital.[20] The rhombicity seems to depend on the balance between small contributions to the singly occupied molecular orbital and whether a simple relation to the structure of the copper site can be formulated remains to be seen.

Concluding Remarks

The complete ***g*** tensor of the type 1 site has been determined from W-band EPR spectroscopy on a single crystal of the green nitrite reductase of *A. faecalis*. The principal *z* axis of this tensor makes an angle of 71° with the CuNN plane and of 60° with the Cu−Sδ(Met 150) direction. Such data are also available for plastocyanin, azurin, M121Q azurin, and M121H azurin, and a model has been formulated that rationalizes the orientation of the *z* axis of the *g* tensor for the type 1 sites in these proteins. The model allows the prediction of the orientation of the *z* axis and of the copper 3d orbital in the singly occupied molecular orbital provided that the structure of the copper site is known. The relation between the rhombicity and the geometry of the copper site of type 1 proteins is not yet fully understood. It remains to be seen whether the slight increase in rhombicity for *A. faecalis* nitrite reductase compared with azurin derives from admixture of the d_{z2} orbital into the wave function of the unpaired electron or from admixture of d_{yz} (d_{xz}) and d_{x2-y2} character.

Acknowledgment. This work has been performed under the auspices of the Biomac Research School of the Leiden and Delft Universities and was supported with financial aid by The Netherlands Organization for Scientific Research (NWO), department Chemical Sciences (CW). Funding to M.E.P.M. was

provided by the National Science and Engineering Research Council (NSERC). M.J.B. is the recipient of a University Graduate Fellowship, and M.E.P.M. is a Medical Research Council of Canada Scholar.

References and Notes

(1) Adman, E. T. In *Topics in Molecular and Structural Biology;* Harrison, P. M., Ed.; Metalloproteins, Vol. 1; MacMillan: New York, 1986; pp 1−42.

(2) Suzuki, S.; Deligeer; Yamaguchi, K.; Kataoka, K.; Kobayashi, K.; Tagawa, S.; Kohzuma, T.; Shidara, S.; Iwasaki, H. *JBIC* **1997**, *2*, 265−274.

(3) Dodd, F. E.; van Beeumen, J.; Eady, R. R.; Hasnain, S. S. *J. Mol. Biol.* **1998**, *282*, 369−382.

(4) Godden, J. W.; Turley, S.; Teller, D. C.; Adman, E. T.; Liu, M. Y.; Payne, W. J.; Legall, J. *Science* **1991**, *253*, 438−442.

(5) Murphy, M. E. P.; Turley, S.; Adman, E. T. *J. Biol. Chem.* **1997**, *272*, 28455−28460.

(6) Strange, R. W.; Murphy, L. M.; Dodd, F. E.; Abraham, Z. H. L.; Eady, R. R.; Hasnain, S. S. *J. Mol. Biol.* **1999**, *287*, 1001−1009.

(7) Kukimoto, M.; Nishiyama, M.; Murphy, M. E. P.; Turley, S.; Adman, E. T.; Horinouchi, S.; Beppu, T. *Biochemistry* **1994**, *33*, 5246−5252.

(8) Guss, J. M.; Freeman, H. C. *J. Mol. Biol.* **1983**, *169*, 521−563.

(9) Nar, H.; Messerschmidt, A.; Huber, R.; van de Kamp, M.; Canters, G. W. *J. Mol. Biol.* **1991**, *221*, 765−772.

(10) Penfield, K. W.; Gewirth, A. A.; Solomon, E. I. *J. Am. Chem. Soc.* **1985**, *107*, 4519−4529.

(11) LaCroix, L. B.; Shadle, S. E.; Wang, Y.; Averill, B. A.; Hedman, B.; Hodgson, K. O.; Solomon, E. I. *J. Am. Chem. Soc.* **1996**, *118*, 7755−7768.

(12) Pierloot, K.; de Kerpel, J. O. A.; Ryde, U.; Olsson, M. H. M.; Roos, B. O. *J. Am. Chem. Soc.* **1998**, *120*, 13156−13166.

(13) Boulanger, M. J.; Kukimoto, M.; Nishiyama, M.; Horinouchi, S.; Murphy, M. E. P. *J. Biol. Chem.* **2000**, *275*, 23957−23964.

(14) Disselhorst, J. A. J. M.; van der Meer, H.; Poluektov, O. G.; Schmidt, J. *J. Magn. Reson. Ser. A* **1995**, *115*, 183−188.

(15) Coremans, J. W. A.; Poluektov, O. G.; Groenen, E. J. J.; Canters, G. W.; Nar, H.; Messerschmidt, A. *J. Am. Chem. Soc.* **1994**, *116*, 3097−3101.

(16) Coremans, J. W. A.; Poluektov, O. G.; Groenen, E. J. J.; Warmerdam, G. C. M.; Canters, G. W.; Nar, H.; Messerschmidt, A. *J. Phys. Chem.* **1996**, *100*, 19706−19713.

(17) Gewirth, A. A.; Solomon, E. I. *J. Am. Chem. Soc.* **1988**, *110*, 3811−3819.

(18) LaCroix, L. B.; Randall, D. W.; Nersissian, A. M.; Hoitink, C. W. G.; Canters, G. W.; Valentine, J. S.; Solomon, E. I. *J. Am. Chem. Soc.* **1998**, *120*, 9620−9631.

(19) Palmer, A. E.; Randall, D. W.; Xu, F.; Solomon, E. I. *J. Am. Chem. Soc.* **1999**, *121*, 7138−7149.

(20) van Gastel, M.; Canters, G. W.; Krupka, H.; Messerschmidt, A.; de Waal, E. C.; Warmerdam, G. C. M.; Groenen, E. J. J. *J. Am. Chem. Soc.* **2000**, *122*, 2322−2328.

(21) Romero, A.; Hoitink, C. W. G.; Nar, H.; Huber, R.; Messerschmidt, A.; Canters, G. W. *J. Mol. Biol.* **1993**, *229*, 1007−1020.

(22) Messerschmidt, A.; Prade, L.; Kroes, S. J.; Sanders-Loehr, J.; Huber, R.; Canters, G. W. *Proc. Natl. Acad. Sci. U.S.A.* **1998**, *95*, 3443−3448.

(23) Wijma, H. J., et al. Unpublished work.

(24) Pierloot, K.; de Kerpel, J. O. A.; Ryde, U.; Roos, B. O. *J. Am. Chem. Soc.* **1997**, *119*, 218−226.

(25) Larsson, S.; Broo, A.; Sjölin, L. *J. Phys. Chem.* **1995**, *99*, 4860−4865.

(26) de Kerpel, J. O. A.; Pierloot, K.; Ryde, U.; Roos, B. O. *J. Phys. Chem. B* **1998**, *102*, 4638−4647.

(27) Gewirth, A. A.; Cohen, S. L.; Schugar, H. J.; Solomon, E. I. *Inorg. Chem.* **1987**, *26*, 1133−1146.